JBC Papers in Press. Published on April 18, 2016 as Manuscript M116.717652
The latest version is at http://www.jbc.org/cgi/doi/10.1074/jbc.M116.717652

Inhibition of Proteasome Activity Induces Formation of Alternative Proteasome Complexes

Vanessa Welk[1], Olivier Coux[2], Vera Kleene[1], Claire Abeza[2], Dietrich Truembach[3], Oliver Eickelberg[1], Silke Meiners[1]*

[1]Comprehensive Pneumology Center (CPC), University Hospital, Ludwig-Maximilians University, Helmholtz Zentrum Muenchen, Munich, Member of the German Center for Lung Research (DZL), Germany.

[2]Centre de Recherche de Biochimie Macromoléculaire (CRBM-CNRS UMR 5237), Université de Montpellier, Montpellier, France

[3]Institute of Developmental Genetics, Helmholtz Zentrum Muenchen, Neuherberg, Germany

*Corresponding author: Silke Meiners, Max-Lebsche Platz 31, 81377 Munich, Germany, Phone: 00498931874673, Fax: 0049893187194673, mail: silke.meiners@helmholtz-muenchen.de

Keywords: proteasome, protein degradation, proteolysis, proteostasis, enzyme inhibitor, PA200, PA28γ

Running title: Induction of Alternative Proteasome Complexes

ABSTRACT

The proteasome is an intracellular protease complex consisting of the 20S catalytic core and its associated regulators, including the 19S complex, PA28αβ, PA28γ, PA200 and PI31. Inhibition of the proteasome induces autoregulatory *de novo* formation of 20S and 26S proteasome complexes. Formation of alternative proteasome complexes, however, has not been investigated so far.

We here show that catalytic proteasome inhibition results in fast recruitment of PA28γ and PA200 to 20S and 26S proteasomes within 2-6 h. Rapid formation of alternative proteasome complexes did not involve transcriptional activation of PA28γ and PA200 but rather recruitment of preexisting activators to 20S and 26S proteasome complexes. Recruitment of proteasomal activators depended on the extent of active site inhibition of the proteasome with inhibition of β5 active sites being sufficient for inducing recruitment. Moreover, specific inhibition of 26S proteasome activity via siRNA-mediated knockdown of the 19S subunit Rpn6 induced recruitment of only PA200 to 20S proteasomes whereas PA28γ was not mobilized.

Here, formation of alternative PA200 complexes involved transcriptional activation of the activator. Alternative proteasome complexes persisted when cells had regained proteasome activity after pulse exposure to proteasome inhibitors. Knockdown of PA28γ sensitized cells to proteasome inhibitor-mediated growth arrest. Thus, formation of alternative proteasome complexes appears to be a formerly unrecognized but integral part of the cellular response to impaired proteasome function and altered proteostasis.

INTRODUCTION

The proteasome, one of the main proteolytic systems of the cell, is essential for maintenance of protein homeostasis and thus of cellular functions. The proteolytic activity of this multicatalytic protease resides inside the 20S core particle, built of four stacked rings of seven α and β subunits with $\alpha_7\beta_7\beta_7\alpha_7$ organization. The internal cavity of the complex, defined by the two β rings, encloses three pairs of distinct active sites named according to their differential cleavage site specificity: chymotrypsin-like (CT-L), trypsin-like (T-L) and caspase-like (C-L) catalytic sites (1). Due to the

closed conformation of the native 20S core complex, binding of different proteasome activators is required to induce opening of the 20S entry pores and allow injection of substrates into the catalytic chamber for degradation (2, 3). Three different families of activators, highly conserved during evolution, have been identified (4): the 19S regulatory particle recognizes polyubiquitylated proteins and targets them for degradation in an ATP-dependent manner (5). Binding of either one or two 19S regulators to the 20S core gives rise to the 26S and 30S proteasome, respectively. The proteasome activator 28 (PA28) family, which comprises the heptameric PA28α/β and PA28γ complexes, and the proteasome activator 200 (PA200), however, function in an ubiquitin- and ATP-independent manner unless they assemble into so-called hybrid proteasome complexes that also contain one 19S regulator attached to one side of the 20S core (3, 6–9). In addition to these three activators, another regulator (PI31) of the 20S complex has been identified but its functions for proteolysis remain obscure (10).

Formation of PA28α/β heteroheptamers is induced by interferon-γ and LPS stimulation of cells. This activator is cytoplasmic and preferentially binds to the inducible 20S immunoproteasome (11–14). Both PA28γ and PA200 are constitutively expressed in most cell types (7, 15). PA28γ is exclusively found in the nucleus and associates as a homoheptamer with the 20S complex (16, 17). PA28γ-containing proteasomes have been implicated in degradation of specific nuclear substrates involved in regulation of cell cycle progression and intranuclear dynamics (6, 18–21). The monomeric PA200 is mainly present in the nucleus (7). Its function is not well understood, but involvement in genomic stability, maintenance of glutamine homeostasis, and spermatogenesis has been reported (22–26).

Recruitment of proteasomal activators to the 20S catalytic core gives rise to a variety of different alternative proteasome complexes consisting of singly or doubly capped 20S proteasomes as well as hybrid complexes of different activators attached to 26S proteasomes (23, 27–29). Recent evidence indicates that the 20S and its activators may function as building blocks that assemble rapidly into different proteasome complexes with diverse functions and substrate specificities, allowing fast and dynamic adaptation of proteasome activity to cellular needs (30–32). Adaptation of 20S and 26S proteasome function has been particularly well studied in response to proteasome inhibition. Inactivation of the 20S catalytic sites by small molecule inhibitors results in concerted transcriptional upregulation of proteasomal genes and augmented formation of 20S and 26S/30S proteasome complexes (33). Moreover, inhibition of 26S proteasomes by silencing of 19S regulatory subunits caused enhanced transcription of proteasomal genes and increased formation of 20S proteasomes in *Drosophila* (34). Recent publications suggested a protective effect of 19S reduction in response to catalytic proteasome inhibition, but involvement of the proteasome activators PA28γ and PA200 in this response has not been investigated so far (35, 36). Recruitment of PA28αβ in response to proteasome inhibition has been shown in reticulocytes lysates *in vitro* (29). Here, we show a so far unknown dynamic recruitment of PA28γ and PA200 to 20S and 26S proteasomes in cells in response to either proteolytic inhibition or siRNA-mediated 26S/30S proteasome knockdown.

EXPERIMENTAL PROCEDURES

Primary cell culture

Primary human lung fibroblasts (phLF) were isolated from organ donor lungs and cultured as previously described (37–39). 24 h prior to treatment phLF were synchronized by incubation in starvation medium containing 1% FBS. Cells were treated with bortezomib (Millennium, Takeda), oprozomib (Onyx Pharmaceuticals) and epoxomicin (APExBIO) at the indicated concentrations and times.

Gene silencing

Knockdown of Rpn6 and PA28γ was performed by reverse transfection of Rpn6 siRNA (*Silencer*® Select s11413, Ambion, Life Technologies), PA28γ siRNAs (*Silencer*® Select s19871 and s19873, Ambion, Life Technologies) or scrambled siRNAs (*Silencer*® Select Negative Control No. 1, 4390843, and Negative Control No. 2, 4390847, Ambion, Life Technologies) at a final concentration of 0.5 nM for Rpn6 silencing and 2 nM for PA28γ silencing using Lipofectamine RNAiMAX (13778150, Life Technologies) as previously reported (39).

Native gel analysis of cell lysates
phLF were lysed in TSDG buffer (50 mM Tris/HCl pH 7.0, 10 mM NaCl, 1.1 mM $MgCl_2$, 0.1 mM EDTA, 1 mM NaN_3, 1 mM DTT, 2 mM ATP, 10% (v/v) glycerol) with complete protease inhibitor cocktail (11697498001, Roche) by seven freezing and thawing cycles in liquid nitrogen. Lysates were centrifuged at maximum speed for 20 min at 4°C and subjected to electrophoresis using the XCell SureLock® Mini-Cell system (EI0001, Life Technologies). 15 µg of protein were run on 3-8% Tris acetate gradient gels (EA0378BOX, Life Technologies) for 3-4 h at 150 V. Chymotrypsin-like activity was monitored as described previously (39). After denaturing in solubilization buffer (2% (w/v) SDS, 66 mM Na_2CO_3, 1.5% β-mercaptoethanol) proteasome complexes were blotted under normal conditions.

Western blot analysis
Cells were lysed in TSDG or RIPA buffer as previously reported (40). Protein concentration was determined by Pierce BCA Protein Assay Kit (10056623, Life Technologies). SDS-PAGE and Western blotting was performed as described before (41). Membranes were incubated overnight at 4°C with one of the following antibodies against PA28γ (sc-136025, 1:1000, Santa Cruz Biotechnology; BML-PW8190-0100, 1:2000, Enzo Life Sciences), PA200 (NBP2-22236, 1:3000, Novus Biologicals), 20S subunit α4 (BML-PW8120, 1:2000, Enzo Life Sciences), 20S subunit β5 (ab90867, 1:1000, Abcam), proteasome 20S α1-7 (ab22674, 1:1000, Abcam), Lys48 specific Ubiquitin (05-1307, 1:1000, Merck Millipore), 19S subunit Rpt5 (A303-538A, 1:5000, Bethyl Laboratories), 19S proteasome subunit Rpn6 (NBP1-46191, 1:2000, Novus Biologicals), Cyclin D1 (2978, 1:500, Cell Signaling) and p21 (MAB88058, 1:3000, Merck Millipore). β-Actin HRP (A3854, 1:80 000, Sigma-Aldrich) was used to monitor equal protein loading and for subsequent normalization of densitometric signals. HRP-linked anti-mouse IgG (7076S, 1:40 000, Cell Signaling) and anti-rabbit IgG antibodies (7074S, 1:40 000, Cell Signaling) as well as Protein G HRP (10-1223, 1: 30 000, Life Technologies) were used for detection using the Amersham ECL Prime Western Blotting Detection Reagent (RPN2232, GE Healthcare). Densitometric analysis in the linear range of exposure was performed and is presented for the protein of interest relative to the respective β-actin protein level.

Gel filtration assay
HeLa cells grown in DMEM (Lonza) containing 4.5 g/l glucose, 10% heat inactivated fetal bovine serum (Biowest), 2 mM glutamine, 100 U/ml penicillin and 10 mg/ml streptomycin (Lonza), treated or not with 10 nM bortezomib for 24 h, were harvested, washed with PBS and kept frozen at -80 °C. Cells were lysed for 10 min at 4 °C in 50 mM Tris-HCl (pH 8.0), 0.5% Igepal CA-630, 5 mM $MgCl_2$, 0.5 mM EDTA, 10% (v/v) glycerol, 50 mM NaCl, 1 mM ATP, 1 mM DTT. After centrifugation (15 min, 4 °C), the extract was filtered (0.2 µm) using a Microspin Filter CA/1.9 Receiver (5000 rpm, 5 min, 4 °C) and 50 µL were loaded on a Superose 6 PC 3.2/30 equilibrated with 50 mM Tris-HCl pH 8.0, 5 mM $MgCl_2$, 0.5 mM EDTA, 10% (v/v) glycerol, 50 mM NaCl, 1 mM ATP, 1 mM DTT. Fractions were resolved by 12% SDS-PAGE and blotted on a PVDF FL membrane (100 V, 90 min). The proteins of interest were immunoprobed using anti-Rpt6 (BML-PW9265, 1:1000, Enzo Life Sciences), anti-β2 (BML-PW8145, 1:1000, Enzo Life Sciences) and anti-PA28γ (611180, 1:1000, BD Biosciences) antibodies, detected using an Odyssey scanner (Licor) and fluorescence was quantified using either the Odyssey or ImageJ software.

Co-immunoprecipitation
Cells were lysed in TSDG buffer as described above. 3 µL of antibody specific for 20S subunit α4 (BML-PW8120, Enzo Life Sciences) were incubated with Protein G magnetic beads (Dynabeads, Thermo Fisher Scientific) for 15 min at 1200 rpm. For immunoprecipitation, 100 µg of protein were incubated with antibody-coupled beads at a total volume of 250 µL for 2 h on an overhead shaker at 4°C. 10 % of the total volume was removed as input control. After four times washing of the beads in 400 µL TSDG buffer containing 0.2% NP40 co-immunoprecipitated proteins were eluted by incubation of beads in Laemmli buffer at 95°C for 10 min. Subsequently, eluted samples and input control were analyzed by SDS-PAGE and Western blotting.

Quantitative real-time RT-PCR
RNA extraction from phLF using Roti®-Quick-Kit (Carl Roth), reverse transcription and quantitative PCR was performed as previously described (40). The 60S ribosomal protein L19 (Rpl19) served as a housekeeping gene for relative expression analysis.

Proteasome activity assay
Proteasome activity was analyzed using fluorescent substrates specific for the chymotrypsin-like (Suc-LLVY-AMC, I-1395, Bachem), caspase-like (Z-Leu-Leu-Glu-AMC, I-1945, Bachem) and trypsin-like activities (Bz-Val-Gly-Arg-AMC, I-1085, Bachem). TSDG protein lysate (2 µg protein for chymotrypsin-like activity and 7 µg for caspase- and typsin-like activity) were subjected to a black flat bottom 96-well plate (Greiner bio-one). Assay buffer (225 mM Tris, 45 mM KCl, 7.5 mM Mg acetate, 7.5 mM $MgCl_2$, 0.2 U creatine phosphokinase, 5 mM phosphocreatine, 6 mM ATP and 1 mM DTT) and 200 µM of the respective substrate was added and incubated for 1 h at 37°C. Fluorescence intensity was measured using a TriStar LB 941 plate reader (Berthold Technologies).

MTT assay
Metabolic activity of phLF in response to PA28γ silencing and bortezomib treatment was analyzed by 2,5-diphenyltetrazolium bromide (MTT) assay. 20 000 cells per well were cultured in a 24-well plate with transfection mixture for PA28γ silencing. After 24 h medium was exchanged to starvation medium containing 1% FBS. 48 h after silencing cells were treated with 10 nM bortezomib for 6 h. Cells were washed with fresh starvation medium and incubated for 24 h to allow recovery of the proteasome activity. For the MTT assay, the cells were incubated with a solution of thiazolyl blue tetrazolium bromide (5 mg/mL in PBS, Sigma) for 1 h at 37°C. Afterwards medium was aspirated and the blue crystals were dissolved in isopropanol + 0.1% Triton X-100. Absorbance was measured at 570 nM in a Sunrise™ plate reader (TECAN).

Cell count
For analysis of cell growth via cell count the same protocol was used as described for the MTT assay with the only difference that cells were cultured in 6-well-plates. Cells were trypsinized, mixed with trypan blue (Sigma-Aldrich) and cell number was determined using a Neubauer counting chamber.

Bioinformatics
All sequences were derived from the promoter sequence retrieval database ElDorado 12-2013 (Genomatix) which is based on NCBI build 37. Promoter sequences of PSME4 (PA200) and PSME3 (PA28γ) from six different species were aligned with the DiAlign TF program (42) in the Genomatix software suite GEMS Launcher to evaluate overall promoter similarity and to identify conserved NRF1 (i.e. Nuclear Factor, Erythroid 2-Like 1 (NFE2L1)) binding sites. The corresponding position weight matrix V$TCF11MAFG.01 was applied to promoter analyses according to the Matrix Family Library Version 9.2 (October 2014). The promoter sequences were defined as in ElDorado. The following Genomatix / Entrez Gene identifier were used for PSME4: GXP_90931 / 23198 (human); GXP_4967564 / 459229 (chimp); GXP_4841060 / 716580 (rhesus monkey); GXP_4346524 / 103554 (mouse); GXP_4713352 / 498433 (rat); GXP_3358724 / 100379940 (western clawed frog). For PSME3 the corresponding identifiers were used: GXP_122956 / 10197 (human); GXP_4318479 / 740582 (chimp); GXP_1055457 / 711900 (rhesus monkey); GXP_31562 / 19192 (mouse); GXP_162448 / 287716 (rat); GXP_3367214 / ENSXETG00000012591 (western clawed frog). Binding sites were considered as conserved when the promoter sequences could be aligned in the region of the NRF1 binding site with help of the DiAlign TF program (using default settings).

Production and purification of PA28γ
The PA28γ (human) cDNA was subcloned into the pET-14B plasmid. After expression in E. coli, the protein complex was purified essentially as previously described for PA28αβ (43).

In vitro reconstitution assay
Purified recombinant PA28γ was mixed with 1 µg of human 20S proteasome (purified from HeLa cells (43) and treated with 25 µM epoxomicin or solvent) in activity buffer (Tris-HCl 20 mM, NaCl 50 mM, DTT 1 mM, glycerol

10%) (final volume 20 µL). After incubation at 37°C for 5 min, the samples were loaded onto a native gel as described (44). After electrophoresis, the gel was incubated with 100 µM Suc-LLVY-AMC in activity buffer at 37°C for 20 min to visualize peptidase activity (44). The gel was then transferred on a PVDF FL membrane (40 V, overnight) and the 20S proteasome and PA28γ were immunoprobed simultaneously with mouse anti-α7 (BML-PW8110-0100, Enzo Life Sciences) and rabbit anti-PA28γ (BML-PW8190-0100, Enzo Life Sciences), respectively. The membrane was scanned using an Odyssey scanner (Licor) and the fluorescence was quantified using the ImageJ software.

Statistical analysis

Statistical analysis was performed using GraphPad Prism 5. Tests used are indicated in the respective figure legends. *P*-values < 0.05 were considered statistically significant (**P* < 0.05, ***P* < 0.01, ****P* < 0.001). Data represent mean +/- SEM.

RESULTS

Catalytic proteasome inhibition induces formation of alternative proteasome complexes.

Primary human lung fibroblasts (phLF) were treated with a single dose of the proteasome inhibitor bortezomib (BZ, 10 nM) for 24 h and formation of proteasome complexes was analyzed via native gel electrophoresis. In-gel activity assays with a specific substrate for the chymotrypsin-like (CT-L) activity demonstrated effective inhibition of 20S and 26S/30S proteasome complexes (Figure 1). Subsequent immunoblotting for α1-7 20S subunits and the 19S subunit Rpt5 unambiguously identified the distinct proteasomes as 20S and 26S/30S complexes, respectively. Blotting of 20S α-subunits also revealed the formation of additional 20S-containing proteasome complexes of higher molecular weight suggesting recruitment of proteasomal activators. Indeed, immunostaining of native gels for PA28α, PA28γ and PA200 proteasome activators demonstrated formation of alternative proteasome complexes, composed of 20S and 26S proteasomes bound to these activators, in response to proteasome inhibitor treatment.

Proteasome activators PA28γ and PA200 are rapidly recruited to 20S and 26S complexes upon proteasome inhibition.

To determine the kinetics of activator recruitment, formation of alternative proteasome complexes was analyzed upon treatment with 10 nM BZ for 2, 6, 16 and 24 h, focusing on the activators PA28γ and PA200. Immunoblotting for the 20S subunit β5 indicated formation of additional 20S containing proteasome complexes at early time points of 2 to 6 h after addition of the proteasome inhibitor (Figure 2A). Indeed, recruitment of PA28γ and PA200 to 20S and 26S proteasomes was observed already after 2 h whereas non-treated controls exhibited low levels of alternative proteasome complexes. Assembly of alternative proteasome complexes increased further over time peaking after 16 h of BZ treatment. Measuring the three different catalytic activities of the proteasome with synthetic fluorescent substrates revealed an almost complete inhibition of the CT-L activity after only 2 h of treatment (Figure 2B). The caspase-like (C-L) active sites were inhibited to a much lesser extent (by 10-40%) than the CT-L activity and with a delayed kinetic. In contrast, the trypsin-like (T-L) activity was significantly elevated after 6 h and peaked at 16 h of inhibitor treatment. Taken together, inhibition of mainly the chymotrypsin-like activity induced rapid and pronounced formation of alternative proteasome complexes.

Proteasomal activators interact with 20S and 26S forming alternative proteasome complexes.

We confirmed our results on the proteasome inhibitor-induced formation of alternative proteasome complexes by two other methods, namely gel filtration and co-immunoprecipitation. Increased binding of PA28γ to 20S and 26S proteasomes was observed in gel filtration assays of BZ-treated HeLa cell extracts and thus confirmed our native gel results in a different cell type (Figure 3A). In solvent treated control cells PA28γ mainly formed free multimers, which were recruited to 20S and 26S complexes in response to proteasome inhibition. Moreover, 20S pull down experiments with an antibody directed against the 20S subunit α4 revealed increased binding of proteasomal activators to the 20S proteasome in phLF upon treatment with 10 nM BZ for 6 h (Figure 3B). Immunoblotting indicated enrichment

of α4 via immunoprecipitation and comparable pulldown efficiencies. Altogether, these data confirm the increased interaction of the activators to 20S proteasomes complexes upon catalytic inhibition of the proteolytic sites in different cell types.

Early recruitment of proteasomal activators is transcriptionally independent.

To investigate the underlying mechanism of recruitment, we analyzed the expression of PA28γ and PA200 in response to proteasome inhibition. Of note, both PA28γ and PA200 protein levels did not change until 16 h of proteasome inhibition as determined by Western blot analysis of phLF (Figure 4A). Only after longer time points, i.e. after 16 and 24 h, levels of the activators were significantly increased compared to time matched controls. For PA200, this corresponded to delayed induction of RNA transcripts after 16 h while PA28γ mRNA expression was not upregulated suggesting differential transcriptional regulation in response to proteasome inhibition (Figure 4B). Divergent transcriptional regulation of PA200 and PA28γ after proteasome inhibition is supported by in silico promoter analysis of both genes for putative binding sites of NRF1 (nuclear factor (erythroid-derived 2)-like 1) (Figure 4C). NRF1 has been described as the critical transcription factor for regulation of proteasomal gene expression in response to proteasome inhibition (45, 46). A highly conserved NRF1 binding site was identified in close proximity to the transcription start of the PSME4 promoter (gene name of PA200). In contrast, only one NRF1 binding site which is only conserved in primates was predicted far upstream of the transcriptional start site of the PSME3 promoter (gene name of PA28γ). These data thus support an early, transcriptionally independent recruitment of preexisting PA28γ and PA200 activators to 20S and 26S proteasome complexes as part of a rapid cellular response to catalytic proteasome inhibition. At later time points, expression of both PA28γ and PA200 is upregulated on the protein level. Only PA200, however, is regulated on the transcriptional level, in a manner possibly involving NRF1.

Inhibition of 26S/30S-proteasome activity induces formation of only PA200 alternative proteasomes.

To further assess whether formation of alternative proteasome complexes and induction of PA28γ and PA200 expression at later time points involves ubiquitin-mediated protein degradation, we selectively inhibited 26S/30S ubiquitin-mediated protein degradation by partial knockdown of the 19S subunit Rpn6 (39, 47, 48).

After 72 h of Rpn6 silencing, we noted marked upregulation of PA200 on mRNA as well as on protein levels whereas expression of PA28γ was not significantly altered (Figures 5A & B). Accumulation of K48-linked polyubiquitylated proteins proved efficient inhibition of ubiquitin-mediated protein degradation by partial knockdown of Rpn6 (Figure 5B). In-gel activity and immunodetection of 20S and 19S subunits confirmed impaired assembly of 26S and 30S complexes (Figure 5C). At the same time, the amount of active 20S was increased and alternative 20S proteasome complexes were formed. Of note, these alternative complexes contained only PA200 but not PA28γ as demonstrated by Western blotting of the native gels. These data further support the notion that delayed transcriptional regulation and alternative proteasome formation is specific for PA200 and involves factors that are sensitive to impairment of ubiquitin-mediated protein degradation such as NRF1, while PA28γ is regulated by mechanisms independent of 26S/30S proteasome activity.

Recruitment of proteasomal activators depends on the extent of proteasome inhibition.

In a next step, we investigated whether acute formation of alternative proteasome complexes directly correlates with the degree of proteasome inhibition. Treatment of phLF with increasing doses of BZ for 6 h (1, 10, 50, 100 nM) led to a dose-dependent inhibition of the CT-L and C-L catalytic sites whereas the T-L like activity was not inhibited. We observed dose-dependent accumulation of alternative proteasomes as shown by native gel electrophoresis and immunoblotting for PA28γ and PA200 (Figure 6A). The small molecule inhibitor oprozomib (OZ) was used to only inhibit the chymotrypsin-like activity of the proteasome (Figure 6B) (49). Again, dose dependent inhibition of the CT-L catalytic site

resulted in enhanced recruitment of PA28γ and PA200 to 20S and 26S proteasomes. Interference with total proteasome activity by treatment with proteasome inhibitor epoxomicin resulted in an even more pronounced formation of alternative proteasome complexes (Figure 6C). Therefore, these results suggest first that inhibition of the chymotrypsin-like activity is sufficient for recruitment of PA200 and PA28γ and second that formation of alternative proteasome directly correlates with the degree of proteasomal inhibition.

PA28γ recruitment to purified 20S proteasomes does not depend on active site modifications by proteasome inhibitors.

Previous data suggested an allosteric opening of 20S core particles upon active site occupancy by peptidic ligands and allosteric stabilization of the 20S-19S interaction in inhibitor-treated 26S proteasomes (50–53). We thus investigated whether recruitment of PA28γ depended on active-site modification of the 20S proteasome *in vitro*. In an *in vitro* reconstitution assay, purified 20S proteasomes were first inactivated by addition of epoxomicin, and binding of purified PA28γ was investigated. Native gel analysis revealed activation of the CT-L activity upon addition of PA28γ, which was completely blocked by epoxomicin treatment (Figure 7). Immunoblotting of the native gels confirmed formation of PA28γ-containing proteasomes. Importantly, binding of PA28γ to the purified 20S proteasome was not enhanced upon active site inhibition as indicated by quantification of PA28γ-bound 20S proteasomes (Figure 7A). Similar results were obtained using bortezomib instead of epoxomicin, and using PA28γ either in limiting or excess molar ratios compared to the 20S proteasome (data not shown). These data suggest that recruitment of the proteasome activator PA28γ is not induced via allosteric reorganization of 20S core complex *in vitro*.

PA28γ recruitment allows cells to cope with proteasome inhibition.

In order to further investigate the functional role of PA28γ-containing alternative proteasome complexes, we performed recovery experiments where cells were first treated with BZ for 6 h and then allowed to recover in fresh medium for 24 h. In this setting, the chymotrypsin- and caspase-like activities, which had been considerably inhibited in response to 6 h BZ treatment, recovered (Figure 8A). The C-L and T-L active sites even showed increased activity compared to controls. Native gel analysis revealed that the CT-L activity was fully restored in 26S/30S proteasome complexes while 20S complexes were still partially inhibited indicating that activity assays with total extracts are not fully reflecting the differential activity profiles of 26S and 20S proteasome complexes (Figure 8B). Of note, PA28γ-containing 20S proteasome complexes persisted upon recovery of proteasome activity suggesting that these alternative complexes may play a functional role for rescuing cells from proteasome inhibition (Figure 8B). We tested this hypothesis by silencing of PA28γ and analysis of the cellular response to 6 h pulse exposure of BZ and 24 h of recovery. While phLF transfected with control siRNAs recovered well from proteasome inhibition, silencing of PA28γ significantly decreased metabolic activity of bortezomib-challenged cells (Figure 8C). Diminished metabolic activity was accompanied by reduced cell numbers in PA28γ-deficient cells in response to BZ treatment (Figure 8D). Of note, the different treatments did not induce cell death but only significantly affected cell numbers of living cells as determined by trypan-blue exclusion assay (data not shown). These data indicate that loss of PA28γ results in cell cycle arrest. In accordance with these findings, protein levels of cyclin D1, whose timely degradation is required for cell cycle progression, and expression of the cell cycle inhibitor p21, a substrate of PA28γ, were significantly elevated upon loss of PA28γ and BZ treatment compared to its controls (Figure 8E) (19, 54). Although we cannot distinguish whether this increase is due to accumulation of p21 in the absence of functional PA28γ or a secondary effect upon cell cycle arrest, these data indicate that cells become more sensitive to proteasome inhibition upon loss of PA28γ and suggest that

PA28γ-containing alternative proteasome complexes may play an important role in the cellular stress response to impaired proteasome function.

DISCUSSION

Our data demonstrate a novel and rapid regulation of alternative proteasome complex formation upon proteasome inhibition. Earlier studies by our group already unraveled enhanced *de novo* assembly of 20S and 26S proteasomes after catalytic 20S inhibition but regulation of alternative proteasomes in cells has not been investigated so far (33). Here, we show for the first time that preexisting proteasome activators PA28γ and PA200 are rapidly recruited to 20S and 26S proteasomes in response to catalytic inhibition of the proteasome in different cell types. In contrast, only PA200 is recruited upon inhibition of 26S ubiquitin-mediated protein degradation. In this latter case, transcriptional activation of PA200 is observed at late stages. To our knowledge such rapid recruitment of proteasomal activators is a novel finding which has only been described for PA28αβ in rabbit reticulocyte lysates *in vitro* (29).

Two central questions arise from this observation: how are proteasomal activators recruited to 20S and 26S proteasomes and why are alternative proteasome complexes formed in the cell?

As proteasomal activators were rapidly recruited to the 20S and 26S proteasomes before any alteration in their expression levels, this suggests the presence of a reservoir of free PA28γ and PA200 in the cell. Indeed, in untreated cells, we observed low levels of both activators associated with 20S or 26S complexes and PA28γ was mainly found as free heptamers while 20S and 26S proteasomes were mostly present in a PA28γ-free form (Figure 3A). Similarly, Fabre et al. observed that the majority of 20S proteasomes is uncapped and that less than 5% of total 20S is associated with PA28γ and PA200 (14). Moreover, proteasome subunits have been described as stable and long-lived proteins, supporting the presence of a backup pool of proteasomal subunits, which can quickly be regulated upon certain stimuli (55). Hence, this pool of available activators may serve as a reserve of building blocks enabling fast recruitment to 20S and 26S proteasomes upon cellular stimuli such as proteotoxic stress.

Rapid recruitment may involve allosteric effects of inhibited 20S core particles, posttranslational modifications or other cofactors rather than induction of protein levels. In our study, recruitment of PA28γ and PA200 directly correlated with the extent of catalytic inhibition with the inhibition of the β5 active site being sufficient for recruitment. This suggests that the decrease in catalytic activity allosterically regulates the association of the 20S core particle with the activators. An allosteric mechanism was proposed for purified yeast proteasomes where inhibition of the β5 active site stabilized the interaction between 20S and 19S complexes (50). Similarly, active site modifications were proposed to induce conformational changes to PA28 binding-sites in *T. acidophilum* (53). Binding of peptidic proteasome inhibitors to the catalytic active sites has been shown to induce an allosteric conformational shift of the α-subunits that propagates opening of the 20S pore (51, 52). However, we did not observe any effects of catalytic proteasome inhibition on the recruitment of purified PA28γ to 20S proteasomes using an *in vitro* reconstitution assay. In addition, PA200-20S alternative proteasomes were formed upon specific inhibition of 26S/30S proteasomes when 20S active sites are not modified by proteasome inhibitors. The underlying mechanism for recruitment remains to be determined and may involve accumulation of substrates, dynamic posttranslational modifications, competing binding partners and cofactors in a complex cellular environment. Cofactors might also be molecules that prevent recruitment of activators to the 20S core complex under normal conditions, but that dissociate upon proteasome inhibition. A similar mechanism has been shown for the ER resident chaperone immunoglobulin-binding protein (BiP), which binds to ER stress sensor proteins at baseline conditions but is recruited to misfolded proteins upon activation of the unfolded protein response thereby activating the sensors (56).

The cellular response to proteasome inhibition involves transcriptional upregulation of 20S proteasome subunits and certain proteasome activators (57). NRF1 was identified as the critical transcription factor for this type of regulation (45, 46). Accordingly, in silico analysis of the PA200

promoter indicated one potential, highly evolutionary conserved NRF1 binding site close to the transcription start site, whereas only one poorly conserved binding site was detected in the extended promoter region of PA28γ. This more reliable prediction of a NRF1 binding site in the promoter sequence of PA200 compared to PA28γ is well in line with our observed specific transcriptional upregulation of PA200 after 16 h of BZ treatment and after 72 h of Rpn6 silencing, while PA28γ was not regulated on the mRNA level at all. In the cell, a vast pool of free PA28γ heptamers exists (Figure 3A). This may function as a backup reservoir and therefore transcriptional induction might not be required for formation of new alternative proteasome complexes.

What is the function of alternative proteasome complexes in the cell that are formed upon proteasome inhibition?
We reason that recruitment of proteasome activators to the 20S and 26S proteasomes is part of a protective cellular stress response to imbalanced protein homeostasis upon proteasome inhibition (30, 58–60). This notion is supported by the observed increased sensitivity of cells to proteasome inhibition upon silencing of PA28γ. Proteasome activators may recruit distinct substrates for proteasomal degradation thereby facilitating cellular recovery after protein stress. In line with this concept, both, PA28γ and PA200, have been shown to target specific proteins for degradation via the 20S core particle: steroid receptor coactivator-3 (SRC-3), cyclin-dependent kinase inhibitors p16, p19 and p21 as well as the deacteylase Sirt1 have been identified as substrates for PA28γ-containing alternative complexes (6, 19, 20, 54). Moreover, PA28γ was shown to be involved in ubiquitin-dependent proteasomal degradation of p53 (61, 62). PA200 has been speculated to contribute to the degradation of peptides and damaged or misfolded proteins arising from cellular stress, since its binding to the 20S core particle induces opening of its channel and facilitates the entry of substrates (7, 27, 63). So far acetylated core histones are the only specific substrates described for PA200 (26). This raises the exciting possibility that rapid formation of PA28γ- and PA200-containing alternative proteasomes directs proteasomal protein degradation to specific sets of substrates in order to allow the cell to cope with conditions of proteotoxic stress upon proteasome inhibition. It is tempting to speculate that this is part of a conserved stress response to misfolded and damaged proteins.
While proteasome inhibitor treatment of cells may not represent a physiologic condition, it is important to understand the therapeutic effects of proteasome inhibitors as bortezomib (Velcade) and carfilzomib (Kyprolis) are approved drugs for the treatment of multiple myeloma (64, 65). The reduction of 26S proteasome function is a physiologically relevant situation. Impairment of 26S proteasome activity has been reported for aging, (66, 67), neurodegeneration (68), and oxidative stress (69). In these studies, however, formation of alternative proteasome complexes as part of the cellular response to impaired 26S proteasome function was not investigated.

In conclusion, our findings demonstrate rapid remodeling of proteasome complexes and support the building block concept in which proteasome activators rapidly assemble into distinct proteasome complexes according to cellular needs (30). Identification of novel compounds that specifically interfere with PA28γ- or PA200-mediated activation of 20S proteasomes should help to unravel the exact cellular roles of these alternative complexes and may also prove to be suitable to manipulate proteasome subcomplexes in a more specific fashion.

Acknowledgements:
We thank Christina Lukas for excellent technical assistance, Korbinian Berschneider for scientific support, Dr. Catherine Bonne-Andrea for cell cultures, and Martina Korfei and Andreas Guenther for providing primary human lung fibroblasts. Vanessa Welk was funded by the Helmholtz Graduate School "Lung Biology and Disease". This project was supported by the COST Action BM1307 PROTEOSTASIS, the European ITN program "UPSTREAM" and (in part) by the Helmholtz Alliance ICEMED, Imaging and Curing Environmental Metabolic Diseases, through the Initiative and Network Fund of the Helmholtz Association.

Conflict of interest:
The authors declare that they have no conflicts of interest with the contents of this article.

Author contributions:
V.W. and S.M. contributed to conception and design of research; V.W., O.C., V.K., C.A. and D.T. performed experiments; V.W., O.C. analyzed data; V.W., O.C. and S.M. interpreted data; V.W. prepared figures; V.W. and S.M. drafted manuscript; V.W., O.C., D.T., O.E. and S.M. revised manuscript; V.W., C.O., V.K., C.A., D.T., O.E. and S.M. approved final version.

REFERENCES

1. Kish-Trier, E., and Hill, C. P. (2013) Structural biology of the proteasome. *Annu. Rev. Biophys.* **42**, 29–49

2. Groll, M., Bajorek, M., Köhler, A., Moroder, L., Rubin, D. M., Huber, R., Glickman, M. H., and Finley, D. (2000) A gated channel into the proteasome core particle. *Nat. Struct. Biol.* **7**, 1062–1067

3. Stadtmueller, B. M., and Hill, C. P. (2011) Proteasome Activators. *Mol. Cancer Res.* **41**, 8–19

4. Fort, P., Kajava, A. V, Delsuc, F., and Coux, O. (2015) Evolution of proteasome regulators in eukaryotes. *Genome Biol. Evol.* **7**, 1363–79

5. Finley, D. (2009) Recognition and processing of ubiquitin-protein conjugates by the proteasome. *Annu. Rev. Biochem.* **78**, 477–513

6. Li, X., Lonard, D. M., Jung, S. Y., Malovannaya, A., Feng, Q., Qin, J., Tsai, S. Y., Tsai, M.-J., and O'Malley, B. W. (2006) The SRC-3/AIB1 coactivator is degraded in a ubiquitin- and ATP-independent manner by the REGgamma proteasome. *Cell*. **124**, 381–92

7. Ustrell, V., Hoffman, L., Pratt, G., and Rechsteiner, M. (2002) Pa200, a nuclear proteasome activator involved in DNA repair. *EMBO J.* **21**, 3516–3525

8. Rechsteiner, M., and Hill, C. P. (2005) Mobilizing the proteolytic machine: Cell biological roles of proteasome activators and inhibitors. *Trends Cell Biol.* **15**, 27–33

9. Dahlmann, B. (2016) Mammalian proteasome subtypes: Their diversity in structure and function. *Arch. Biochem. Biophys.* **591**, 132–140

10. Li, X., Thompson, D., Kumar, B., and DeMartino, G. N. (2014) Molecular and cellular roles of PI31 (PSMF1) protein in regulation of proteasome function. *J. Biol. Chem.* **289**, 17392–17405

11. Groettrup, M., Soza, a, Eggers, M., Kuehn, L., Dick, T. P., Schild, H., Rammensee, H. G., Koszinowski, U. H., and Kloetzel, P. M. (1996) A role for the proteasome regulator PA28alpha in antigen presentation. *Nature*. **381**, 166–168

12. Dick, T. P., Ruppert, T., Groettrup, M., Kloetzel, P. M., Kuehn, L., Koszinowski, U. H., Stevanović, S., Schild, H., and Rammensee, H. G. (1996) Coordinated dual cleavages induced by the proteasome regulator PA28 lead to dominant MHC ligands. *Cell*. **86**, 253–262

13. Ossendorp, F., Fu, N., Camps, M., Granucci, F., Gobin, S. J. P., van den Elsen, P. J., Schuurhuis, D., Adema, G. J., Lipford, G. B., Chiba, T., Sijts, A., Kloetzel, P.-M., Ricciardi-Castagnoli, P., and

Melief, C. J. M. (2005) Differential expression regulation of the alpha and beta subunits of the PA28 proteasome activator in mature dendritic cells. *J. Immunol.* **174**, 7815–7822

14. Fabre, B., Lambour, T., Garrigues, L., Ducoux-Petit, M., Amalric, F., Monsarrat, B., Burlet-Schiltz, O., and Bousquet-Dubouch, M.-P. (2014) Label-Free Quantitative Proteomics Reveals the Dynamics of Proteasome Complexes Composition and Stoichiometry in a Wide Range of Human Cell Lines. *J. Proteome Res.* **13**, 3027–3037

15. Yu, G., Zhao, Y., He, J., Lonard, D. M., Mao, C.-A., Wang, G., Li, M., and Li, X. (2010) Comparative analysis of REG{gamma} expression in mouse and human tissues. *J. Mol. Cell Biol.* **2**, 192–198

16. Realini, C., Jensen, C. C., Zhang, Z. -g., Johnston, S. C., Knowlton, J. R., Hill, C. P., and Rechsteiner, M. (1997) Characterization of Recombinant REG , REG , and REG Proteasome Activators. *J. Biol. Chem.* **272**, 25483–25492

17. Li, J., and Rechsteiner, M. (2001) Molecular dissection of the 11S REG (PA28) proteasome activators. *Biochimie*. **83**, 373–383

18. Murata, S., Kawahara, H., Tohma, S., Yamamoto, K., Kasahara, M., Nabeshima, Y. -i., Tanaka, K., and Chiba, T. (1999) Growth Retardation in Mice Lacking the Proteasome Activator PA28 . *J. Biol. Chem.* **274**, 38211–38215

19. Li, X., Amazit, L., Long, W., Lonard, D. M., Monaco, J. J., and O'Malley, B. W. (2007) Ubiquitin- and ATP-independent proteolytic turnover of p21 by the REGgamma-proteasome pathway. *Mol. Cell*. **26**, 831–42

20. Dong, S., Jia, C., Zhang, S., Fan, G., Li, Y., Shan, P., Sun, L., Xiao, W., Li, L., Zheng, Y., Liu, J., Wei, H., Hu, C., Zhang, W., Chin, Y. E., Zhai, Q., Li, Q., Liu, J., Jia, F., Mo, Q., Edwards, D. P., Huang, S., Chan, L., O'Malley, B. W., Li, X., and Wang, C. (2013) The REGγ proteasome regulates hepatic lipid metabolism through inhibition of autophagy. *Cell Metab.* **18**, 380–91

21. Baldin, V., Militello, M., Thomas, Y., Doucet, C., Fic, W., Boireau, S., Jariel-Encontre, I., Piechaczyk, M., Bertrand, E., Tazi, J., and Coux, O. (2008) A novel role for PA28gamma-proteasome in nuclear speckle organization and SR protein trafficking. *Mol. Biol. Cell*. **19**, 1706–1716

22. Blickwedehl, J., McEvoy, S., Wong, I., Kousis, P., Clements, J., Elliott, R., Cresswell, P., Liang, P., and Bangia, N. (2007) Proteasomes and proteasome activator 200 kDa (PA200) accumulate on chromatin in response to ionizing radiation. *Radiat. Res.* **167**, 663–74

23. Blickwedehl, J., Agarwal, M., Seong, C., Pandita, R. K., Melendy, T., Sung, P., Pandita, T. K., and Bangia, N. (2008) Role for proteasome activator PA200 and postglutamyl proteasome activity in genomic stability. *Proc. Natl. Acad. Sci. U. S. A.* **105**, 16165–70

24. Blickwedehl, J., Olejniczak, S., Cummings, R., Sarvaiya, N., Mantilla, A., Chanan-Khan, A., Pandita, T. K., Schmidt, M., Thompson, C. B., and Bangia, N. (2012) The proteasome activator PA200 regulates tumor cell responsiveness to glutamine and resistance to ionizing radiation. *Mol. Cancer Res.* **10**, 937–44

25. Khor, B., Bredemeyer, A. L., Huang, C., Turnbull, I. R., Evans, R., Maggi, L. B., White, J. M., Walker, L. M., Carnes, K., Hess, R. A., and Sleckman, B. P. (2006) Proteasome activator PA200 is required for normal spermatogenesis. *Mol. Cell. Biol.* **26**, 2999–3007

26. Qian, M.-X., Pang, Y., Liu, C. H., Haratake, K., Du, B.-Y., Ji, D.-Y., Wang, G.-F., Zhu, Q.-Q., Song, W., Yu, Y., Zhang, X.-X., Huang, H.-T., Miao, S., Chen, L.-B., Zhang, Z.-H., Liang, Y.-N., Liu, S., Cha, H., Yang, D., Zhai, Y., Komatsu, T., Tsuruta, F., Li, H., Cao, C., Li, W., Li, G.-H., Cheng, Y., Chiba, T., Wang, L., Goldberg, A. L., Shen, Y., and Qiu, X.-B. (2013) Acetylation-mediated proteasomal degradation of core histones during DNA repair and spermatogenesis. *Cell*. **153**, 1012–24

27. Ortega, J., Heymann, J. B., Kajava, A. V, Ustrell, V., Rechsteiner, M., and Steven, A. C. (2005) The axial channel of the 20S proteasome opens upon binding of the PA200 activator. *J. Mol. Biol.* **346**, 1221–7

28. Tanahashi, N., Murakami, Y., Minami, Y., Shimbara, N., Hendil, K. B., and Tanaka, K. (2000) Hybrid Proteasomes. *Biochemistry*. **275**, 14336–14345

29. Shibatani, T., Carlson, E. J., Larabee, F., McCormack, A. L., Früh, K., and Skach, W. R. (2006) Global organization and function of mammalian cytosolic proteasome pools: Implications for PA28 and 19S regulatory complexes. *Mol. Biol. Cell*. **17**, 4962–4971

30. Meiners, S., Keller, I. E., Semren, N., and Caniard, A. (2014) Regulation of the proteasome: evaluating the lung proteasome as a new therapeutic target. *Antioxid. Redox Signal.* **21**, 2364–82

31. Schmidt, M., and Finley, D. (2014) Regulation of proteasome activity in health and disease. *Biochim. Biophys. Acta*. **1843**, 13–25

32. Lokireddy, S., Kukushkin, N. V., and Goldberg, A. L. (2015) cAMP-induced phosphorylation of 26S proteasomes on Rpn6/PSMD11 enhances their activity and the degradation of misfolded proteins. *Proc. Natl. Acad. Sci.* 10.1073/pnas.1522332112

33. Meiners, S., Heyken, D., Weller, A., Ludwig, A., Stangl, K., Kloetzel, P.-M., and Krüger, E. (2003) Inhibition of proteasome activity induces concerted expression of proteasome genes and de novo formation of Mammalian proteasomes. *J. Biol. Chem.* **278**, 21517–25

34. Wójcik, C., and DeMartino, G. N. (2002) Analysis of Drosophila 26 S proteasome using RNA interference. *J. Biol. Chem.* **277**, 6188–97

35. Acosta-Alvear, D., Cho, M. Y., Wild, T., Buchholz, T. J., Lerner, A. G., Simakova, O., Hahn, J., Korde, N., Landgren, O., Maric, I., Choudhary, C., Walter, P., Weissman, J. S., and Kampmann, M. (2015) Paradoxical resistance of multiple myeloma to proteasome inhibitors by decreased levels of 19S proteasomal subunits. *Elife*. **4**, e08153

36. Tsvetkov, P., Mendillo, M. L., Zhao, J., Carette, J. E., Merrill, P. H., Cikes, D., Varadarajan, M., van Diemen, F. R., Penninger, J. M., Goldberg, A. L., Brummelkamp, T. R., Santagata, S., and Lindquist, S. (2015) Compromising the 19S proteasome complex protects cells from reduced flux through the proteasome. *Elife*. **4**, 1–22

37. Jordana, M., Newhouse, M. T., and Gauldie, J. (1987) Alveolar macrophage/peripheral blood monocyte-derived factors modulate proliferation of primary lines of human lung fibroblasts. *J. Leukoc. Biol.* **42**, 51–60

38. Jordana, M., Befus, A. D., Newhouse, M. T., Bienenstock, J., and Gauldie, J. (1988) Effect of histamine on proliferation of normal human adult lung fibroblasts. *Thorax*. **43**, 552–558

39. Semren, N., Welk, V., Korfei, M., Keller, I. E., Fernandez, I. E., Adler, H., Günther, A., Eickelberg, O., and Meiners, S. (2015) Regulation of 26S Proteasome Activity in Pulmonary Fibrosis. *Am. J. Respir. Crit. Care Med.* **192**, 1089–1101

40. Keller, I. E., Vosyka, O., Takenaka, S., Kloß, A., Dahlmann, B., Willems, L. I., Verdoes, M., Overkleeft, H. S., Marcos, E., Adnot, S., Hauck, S. M., Ruppert, C., Günther, A., Herold, S., Ohno, S., Adler, H., Eickelberg, O., and Meiners, S. (2015) Regulation of Immunoproteasome Function in the Lung. *Sci. Rep.* **5**, 10230

41. van Rijt, S. H., Keller, I. E., John, G., Kohse, K., Yildirim, a. O., Eickelberg, O., and Meiners, S. (2012) Acute cigarette smoke exposure impairs proteasome function in the lung. *AJP Lung Cell. Mol. Physiol.* **303**, L814–L823

42. Cartharius, K., Frech, K., Grote, K., Klocke, B., Haltmeier, M., Klingenhoff, A., Frisch, M., Bayerlein, M., and Werner, T. (2005) MatInspector and beyond: promoter analysis based on transcription factor binding sites. *Bioinformatics*. **21**, 2933–2942

43. Le Feuvre, A. Y., Dantas-Barbosa, C., Baldin, V., and Coux, O. (2009) High yield bacterial expression and purification of active recombinant PA28alphabeta complex. *Protein Expr. Purif.* **64**, 219–24

44. Glickman, M., and Coux, O. (2001) Purification and characterization of proteasomes from Saccharomyces cerevisiae. *Curr. Protoc. Protein Sci.* **Chapter 21**, Unit 21.5

45. Radhakrishnan, S. K., Lee, C. S., Young, P., Beskow, A., Chan, J. Y., and Deshaies, R. J. (2010) Transcription factor Nrf1 mediates the proteasome recovery pathway after proteasome inhibition in mammalian cells. *Mol. Cell*. **38**, 17–28

46. Steffen, J., Seeger, M., Koch, A., and Krüger, E. (2010) Proteasomal degradation is transcriptionally controlled by TCF11 via an ERAD-dependent feedback loop. *Mol. Cell*. **40**, 147–58

47. Santamaría, P. G., Finley, D., Ballesta, J. P. G., and Remacha, M. (2003) Rpn6p, a proteasome subunit from Saccharomyces cerevisiae, is essential for the assembly and activity of the 26 S proteasome. *J. Biol. Chem.* **278**, 6687–6695

48. Vilchez, D., Boyer, L., Morantte, I., Lutz, M., Merkwirth, C., Joyce, D., Spencer, B., Page, L., Masliah, E., Berggren, W. T., Gage, F. H., and Dillin, A. (2012) Increased proteasome activity in human embryonic stem cells is regulated by PSMD11. *Nature*. **489**, 304–308

49. Dick, L. R., and Fleming, P. E. (2010) Building on bortezomib: second-generation proteasome inhibitors as anti-cancer therapy. *Drug Discov. Today*. **15**, 243–9

50. Kleijnen, M. F., Roelofs, J., Park, S., Hathaway, N. a, Glickman, M., King, R. W., and Finley, D. (2007) Stability of the proteasome can be regulated allosterically through engagement of its proteolytic active sites. *Nat. Struct. Mol. Biol.* **14**, 1180–8

51. Osmulski, P. A., Hochstrasser, M., and Gaczynska, M. (2009) A Tetrahedral Transition State at the Active Sites of the 20S Proteasome Is Coupled to Opening of the ??-Ring Channel. *Structure*. **17**, 1137–1147

52. Arciniega, M., Beck, P., Lange, O. F., Groll, M., and Huber, R. (2014) Differential global structural changes in the core particle of yeast and mouse proteasome induced by ligand binding. *Proc. Natl. Acad. Sci. U. S. A.* **111**, 9479–84

53. Ruschak, A. M., and Kay, L. E. (2012) Proteasome allostery as a population shift between interchanging conformers. *Proc Natl Acad Sci U S A*. **109**, E3454–62

54. Chen, X., Barton, L. F., Chi, Y., Clurman, B. E., and Roberts, J. M. (2007) Ubiquitin-independent degradation of cell-cycle inhibitors by the REGgamma proteasome. *Mol. Cell*. **26**, 843–52

55. Schwanhäusser, B., Busse, D., Li, N., Dittmar, G., Schuchhardt, J., Wolf, J., Chen, W., and Selbach, M. (2011) Global quantification of mammalian gene expression control. *Nature*. **473**, 337–342

56. Ron, D., and Walter, P. (2007) Signal integration in the endoplasmic reticulum unfolded protein response. **8**, 519–529

57. Sha, Z., and Goldberg, A. L. (2014) Proteasome-mediated processing of Nrf1 is essential for coordinate induction of all proteasome subunits and p97. *Curr. Biol.* **24**, 1573–83

58. Meiners, S., Ludwig, A., Lorenz, M., Dreger, H., Baumann, G., Stangl, V., and Stangl, K. (2006) Nontoxic proteasome inhibition activates a protective antioxidant defense response in endothelial cells. *Free Radic. Biol. Med.* **40**, 2232–41

59. Di Napoli, Mario and McLaughlin, BethAnn (2005) The proteasome ubiquitin system as a drug target in cerrebrovascular disease: The therapeutic potencial of proteasome inhibitors. *Curr. Opin. Investig. drugs*. **6**, 686–699

60. Wójcik, C. (1999) Proteasomes in apoptosis: Villains or guardians? *Cell. Mol. Life Sci.* **56**, 908–917

61. Zhang, Z., and Zhang, R. (2008) Proteasome activator PA28 gamma regulates p53 by enhancing its MDM2-mediated degradation. *EMBO J.* **27**, 852–64

62. Liu, J., Yu, G., Zhao, Y., Zhao, D., Wang, Y., Wang, L., Liu, J., Li, L., Zeng, Y., Dang, Y., Wang, C., Gao, G., Long, W., Lonard, D. M., Qiao, S., Tsai, M.-J., Zhang, B., Luo, H., and Li, X. (2010) REGgamma modulates p53 activity by regulating its cellular localization. *J. Cell Sci.* **123**, 4076–84

63. Savulescu, A. F., and Glickman, M. H. (2011) Proteasome activator 200: the heat is on... *Mol. Cell. Proteomics*. **10**, R110.006890

64. Kane, R. C., Farrell, A. T., Sridhara, R., and Pazdur, R. (2006) United States Food and Drug Administration approval summary: Bortezomib for the treatment of progressive multiple myeloma after one prior therapy. *Clin. Cancer Res.* **12**, 2955–2960

65. Herndon, T. M., Deisseroth, A., Kaminskas, E., Kane, R. C., Koti, K. M., Rothmann, M. D., Habtemariam, B., Bullock, J., Bray, J. D., Hawes, J., Palmby, T. R., Jee, J., Adams, W., Mahayni, H., Brown, J., Dorantes, A., Sridhara, R., Farrell, A. T., and Pazdur, R. (2013) U.s. Food and Drug Administration approval: carfilzomib for the treatment of multiple myeloma. *Clin. Cancer Res.* **19**, 4559–63

66. Vernace, V. A., Arnaud, L., Schmidt-Glenewinkel, T., and Figueiredo-Pereira, M. E. (2007) Aging perturbs 26S proteasome assembly in Drosophila melanogaster. *FASEB J.* **21**, 2672–82

67. Tonoki, A., Kuranaga, E., Tomioka, T., Hamazaki, J., Murata, S., Tanaka, K., and Miura, M. (2009) Genetic evidence linking age-dependent attenuation of the 26S proteasome with the aging process. *Mol. Cell. Biol.* **29**, 1095–106

68. Myeku, N., Clelland, C. L., Emrani, S., Kukushkin, N. V, Yu, W. H., Goldberg, A. L., and Duff, K. E. (2015) Tau-driven 26S proteasome impairment and cognitive dysfunction can be prevented early in disease by activating cAMP-PKA signaling. *Nat. Med.* **6**, 1–11

69. Livnat-Levanon, N., Kevei, E., Kleifeld, O., Krutauz, D., Segref, A., Rinaldi, T., Erpapazoglou, Z., Cohen, M., Reis, N., Hoppe, T., and Glickman, M. (2014) Reversible 26S proteasome disassembly upon mitochondrial stress. *Cell Rep.* **7**, 1371–1380

FOOTNOTES

The abbreviations used are: CT-L, chymotrypsin-like; T-L, trypsin-like; C-L, caspase-like; ATP, adenosine triphosphate; PA28, proteasome activator 28; PA200, proteasome activator 200; HRP, horse radish peroxidase; Rpl19, ribosomal protein L19; BZ, bortezomib; OZ, oprozomib; NRF1, nuclear factor erythroid 2-related factor 1; phLF, primary human lung fibroblasts.

FIGURE LEGENDS

Figure 1: Catalytic proteasome inhibition induces formation of alternative proteasome complexes.
Primary human lung fibroblasts (phLF) were treated with 10 nM bortezomib (BZ) for 24 h and native cell lysates were prepared. Active proteasome complexes were resolved by native gel electrophoresis with chymotrypsin-like (CT-L) substrate overlay assay and immunoblotting for 20S α1-7 subunits, 19S subunit Rpt5 and the proteasomal activators PA28α, PA28γ and PA200. Experiments were performed in distinct phLF lines of three different organ donors. Figures indicate representative results of one donor line.

Figure 2: Proteasome activators PA28γ and PA200 are rapidly recruited to 20S and 26S complexes upon proteasome inhibition.
A) Time-dependent response of primary human lung fibroblasts (phLF) to 10 nM bortezomib (BZ) treatment for 2, 6, 16, and 24 h with regard to formation of alternative proteasome complexes as analyzed by native gel electrophoresis. In-gel activity assay shows the CT-L activity of the proteasome complexes. 20S and 26/30S proteasome complexes were detected using the β5 antibody. Association of PA28γ and PA200 with 20S and 26S proteasomes was detected via immunoblotting using the respective antibodies. All experiments were performed in primary human lung fibroblasts from three different organ donors. Native gels indicate representative results of one donor.
B) Proteasome activity assay of chymotrypsin- (CT-L), caspase- (C-L) and trypsin-like (T-L) activities of total cell lysates as used in A). Bars indicate % activity compared to the time matching control for three experiments using three different phLF lines (One-way ANOVA, Bonferroni's Multiple Comparison Test, n=3).

Figure 3: Proteasomal activators interact with 20S/26S proteasomes forming alternative proteasome complexes.
A) Gel filtration assay of PA28γ proteasome complexes in bortezomib (BZ) treated HeLa cells compared to control. Western blot analysis of Rpt5, β2, and PA28γ in the top panel shows representative images of the protein distribution in the different fractions separated by gel filtration. The bottom panel shows the quantification of the signal for PA28γ in BZ treated cells and controls. For clarity, the intensity of the

signal has been normalized to the maximum value of each curve, and the total areas under each curve were made equal.
B) Analysis of interaction of proteasomal activators with the 20S proteasome using co-immunoprecipitation. Lysates of primary human lung fibroblasts (phLF) were treated with BZ for 6 h or with solvent, lysed and subjected to immunoprecipitation using an antibody against the 20S subunit α4. Co-immunoprecipitated proteins as well as total protein lysate (input, 10% of total volume) were separated by SDS-PAGE. Direct interaction of proteasomal activators PA28γ and PA200 with the 20S proteasome subunit α4 was visualized via immunoblotting. Representative results of experiments in cells from three different donors are shown.

Figure 4: Early recruitment of proteasomal activators is transcriptionally independent.
A) Western blot analysis showing expression of total PA28γ and PA200 in primary human lung fibroblasts (phLF) treated with 10 nM bortezomib (BZ) for 2 h, 6 h, 16 h and 24 h and densitometric analysis of β-actin normalized signals relative to time matched untreated controls (One-way ANOVA, Bonferroni's Multiple Comparison Test, n=3).
B) Quantitative RT-PCR analysis of PA28γ and PA200 in phLF in response to 10 nM BZ treatment for 2 to 24 h. Bars indicate fold change of relative mRNA levels compared to time-matched controls (One-way ANOVA, Bonferroni's Multiple Comparison Test, n=3).
C) Promotor analysis of the PSME4 and PSME3 promoter for putative NRF1 binding sites and their conservation in vertebrates. Schematic representation of PSME4 and PSME3 promoter sequences from different species: human (*Homo sapiens*); chimp (*Pan troglodytes*); rhesus monkey (*Macaca mulatta*); mouse (*Mus musculus*); rat (*Rattus norvegicus*); western clawed frog (*Xenopus tropicalis*). The red arrow indicates the transcription start site (TSS) and positions are denoted relative to the TSS. The predicted NRF1 binding sites are indicated by semicircles. Green semicircles represent conserved binding sites whereas grey semicircles indicate not conserved binding sites (above sequence: binding sites on the plus strand; below sequence: binding sites on the minus strand). The PSME4 promoter contains two putative NRF1 binding sites, of which one is conserved in vertebrates. Functional relevance of the putative NRF1 binding site close to the TSS (in the range of -322 bp to +56 bp) within the PSME4 promoter sequences is supported by evolutionary conservation across six vertebrate species. In contrast, for the PSME3 promoter one NRF1 binding site is predicted which is conserved only in primates.

Figure 5: Inhibition of 26S/30S-mediated protein degradation induces formation of only PA200 alternative proteasomes.
A) Primary human lung fibroblasts (phLF) were treated with Rpn6 or scrambled control siRNAs for 72 h and mRNA expression of Rpn6, PA28γ and PA200 upon Rpn6 silencing was assessed by quantitative RT-PCR. Bars indicate fold change of mRNA levels compared to control siRNA-transfected cells (One sample t-Test, n=3).
B) Western blot analysis for K48-polyubiquitylated (UbiK48) proteins, the 19S regulatory subunit Rpn6 and proteasomal activators PA28γ and PA200 in response to Rpn6 knockdown. Densitometric analysis indicates β-actin normalized signals relative to the respective scrambled siRNA control (One sample t-Test, n=3).
C) Native gel analysis of Rpn6 silencing. In-gel CT-L activity assays and immunoblotting for the 19S subunit Rpt5, the 20S subunits α1-7 and PA28γ and PA200 indicate the activity and composition of proteasome complexes. Experiments were performed in phLF from three different organ donors and representative results of one donor are shown.

Figure 6: Recruitment of proteasomal activators depends on the extent of proteasome inhibition.
Primary human lung fibroblasts (phLF) were treated with different doses of proteasome inhibitors (bortezomib (BZ) in A); oprozomib (OZ) in B) for 6 h, lysed and chymotrypsin-like (CT-L), caspase-like (C-L) and trypsin-like (T-L) activities were measured using fluorescent substrates. Bars indicate % activity compared to the solvent treated control for three experiments using three different phLF lines (One-way ANOVA, Bonferroni's Multiple Comparison Test, n=3). Dose dependent recruitment of proteasomal activators was detected via native gel electrophoresis including in-gel CT-L activity assay and immunoblotting for PA28γ and PA200 using the respective antibodies.
C) Analysis of proteasome activity and proteasome complex formation in response to treatment of phLF with 20 μM epoxomicin for 4.5 h. Bars show % activity compared to the solvent treated control. All experiments were performed in phLF from three different organ donors and native gels show representative results of one donor (One-way ANOVA, Bonferroni's Multiple Comparison Test, n=3).

Figure 7: PA28γ recruitment to purified 20S proteasomes does not depend on active site modifications by proteasome inhibitors.
Purified recombinant PA28γ (0 or 2 μg) was mixed with 1 μg of 20S proteasome pretreated on ice with 25 μM epoxomicin (or the same volume of DMSO (vehicle) as control). After incubation at 37°C for 5 min (final volume 20 μL, final concentration of epoxomicin 12.5 μM), the samples were resolved by native gel electrophoresis and the gel was incubated with 100 μM Suc-LLVY-AMC to visualize chymotrypsin-like activity. Formation of PA28γ proteasome complexes was analyzed via immunoblotting for PA28γ and α7. Bar diagram indicates quantification of PA28γ-bound 20S. The 20S proteasome is in a latent state and thus has little activity by itself. Addition of PA28γ results into a large activation of 20S activity, as expected.

Figure 8: PA28γ recruitment allows cells to cope with proteasome inhibition.
A) Analysis of proteasome activity in primary human lung fibroblasts (phLF) after 6 h bortezomib (BZ) treatment and recovery in fresh medium for 24 h by using fluorescent substrates specific for the three catalytic sites of the proteasome. Bars indicate % activity compared to the solvent treated control for three experiments using three different phLF lines (One-way ANOVA, Bonferroni's Multiple Comparison Test, n=3).
B) Analysis of proteasome complex formation of lysates used in A) via native gel analysis including in-gel CT-L activity assay and immunoblotting for 20S subunit β5 and PA28γ using the respective antibody.
C) Metabolic activity of phLF after PA28γ silencing and co-treatment with BZ. 48 h after transient silencing of PA28γ, phLF were treated with 10 nM BZ for 6 h followed by 24 h recovery in fresh medium. Metabolic activity of BZ and siRNA co-treated cells was assessed using the MTT assay. Bars indicate % metabolic activity compared to control siRNA and solvent treated control (One-way ANOVA, Bonferroni's Multiple Comparison Test, n=3).
D) Determination of cell numbers of upon treatment as in C). The number of dead and living cells was determined by trypan blue exclusion. Bar diagram shows % cell count of living cells compared to control siRNA and solvent treated control. The number of dead cells was negligible in all conditions (One-way ANOVA, Bonferroni's Multiple Comparison Test, n=4).
E) Analysis of the accumulation of cyclin D1 and p21 in phLF upon PA28γ silencing and co-treatment with BZ. 48 h after transient silencing of PA28γ, phLF were treated with 10 nM BZ for 6 h followed by 24 h recovery in fresh medium. PA28γ, Cyclin D1 and p21 protein levels were analyzed by Western blotting using the respective antibodies. Bar diagram indicates densitometric analysis of β-actin normalized signals relative to the scrambled siRNA control (One-way ANOVA, Bonferroni's Multiple Comparison Test, n=4).

Figure 1

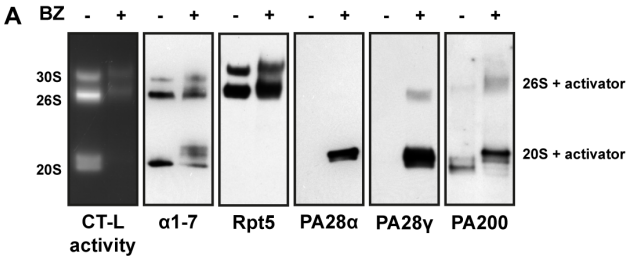

Figure 2

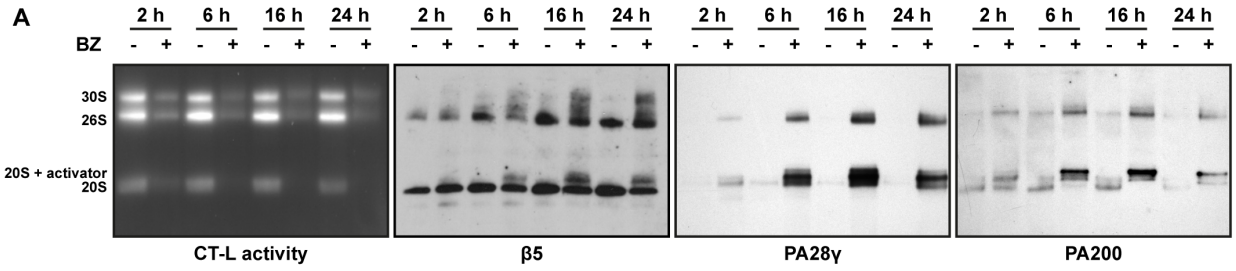

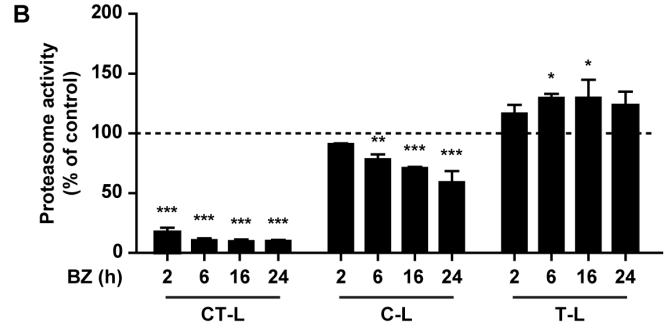

Figure 3

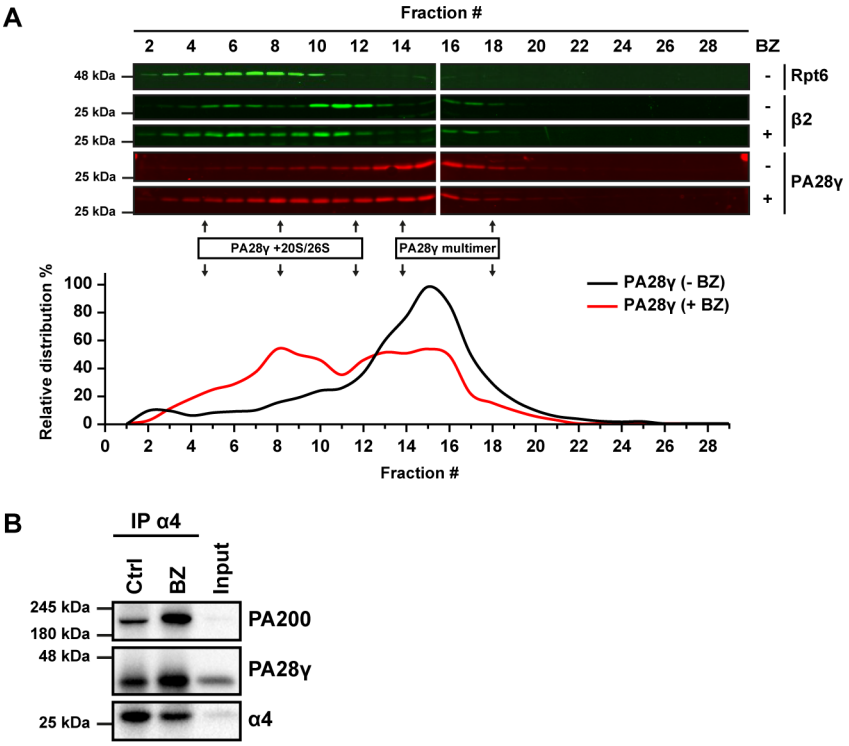

Figure 4

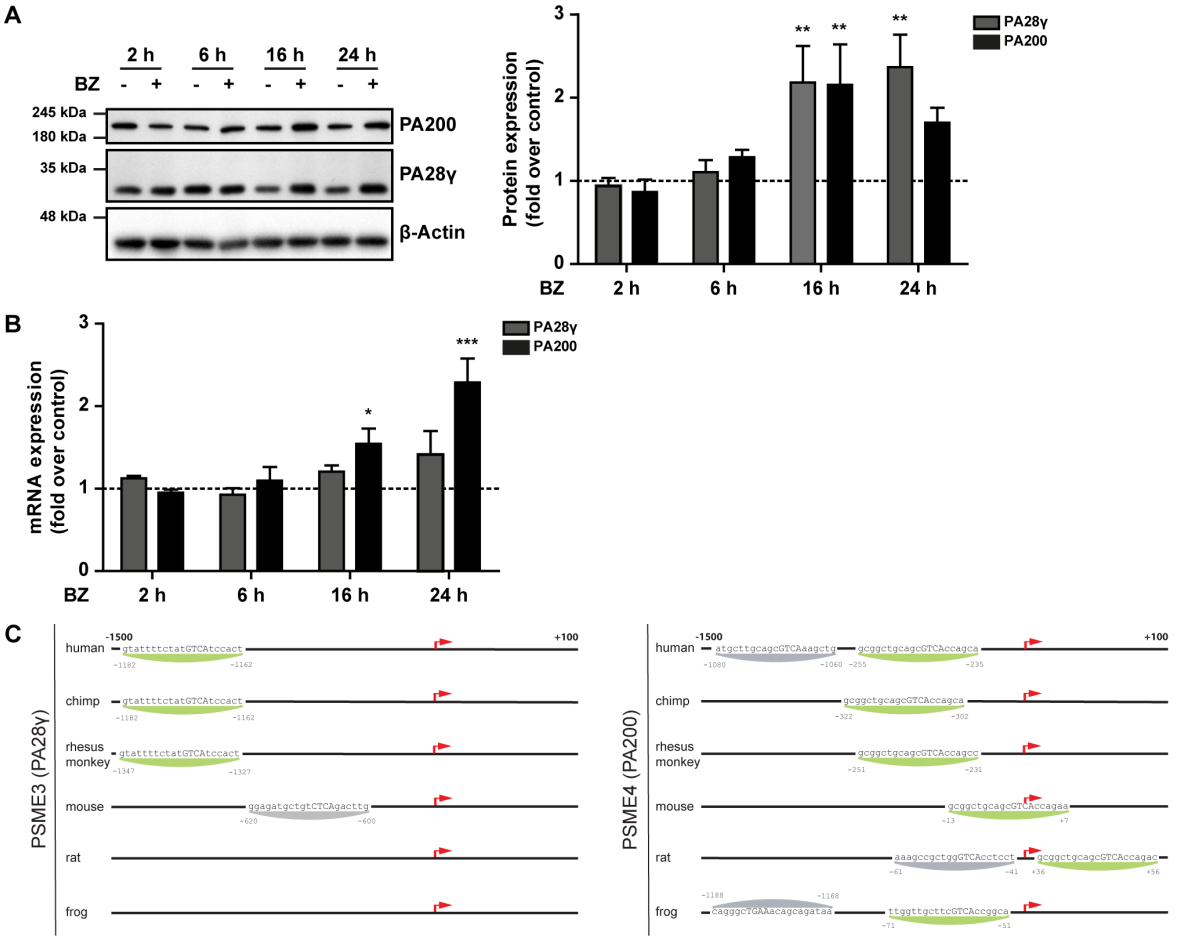

Figure 5

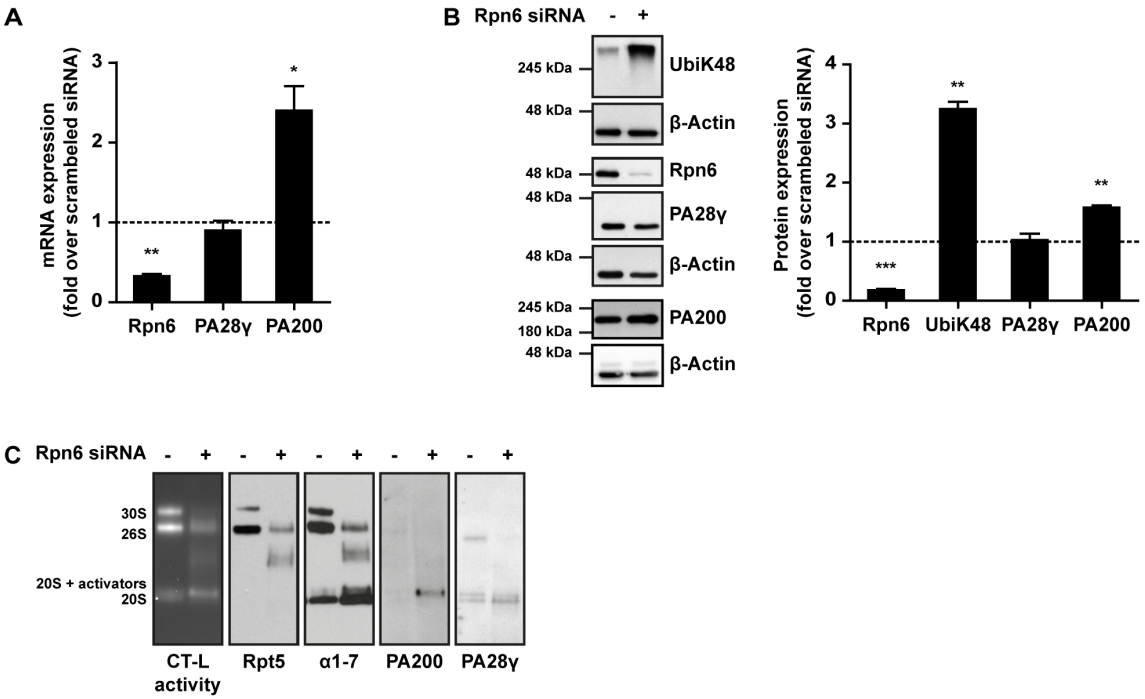

Figure 6

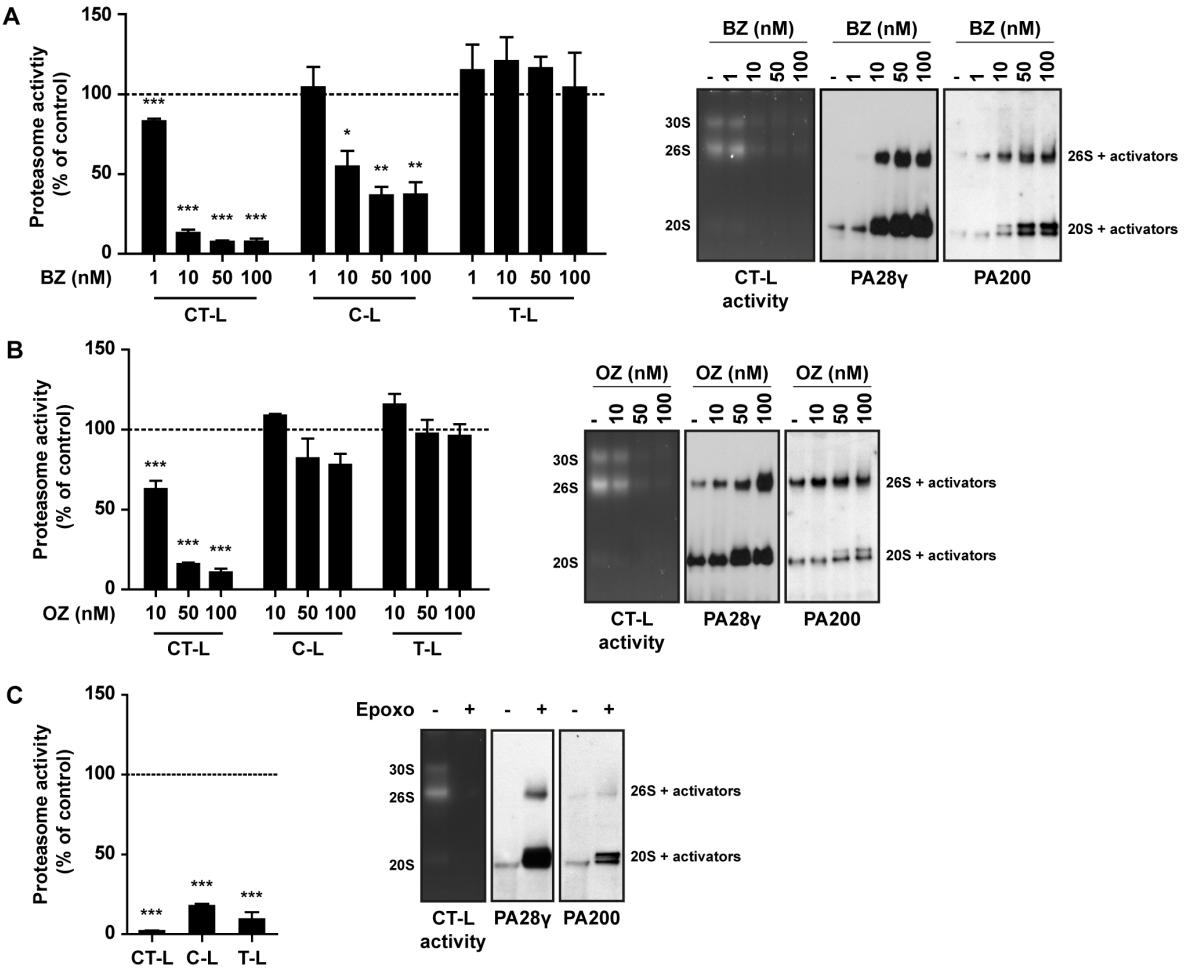

Figure 7

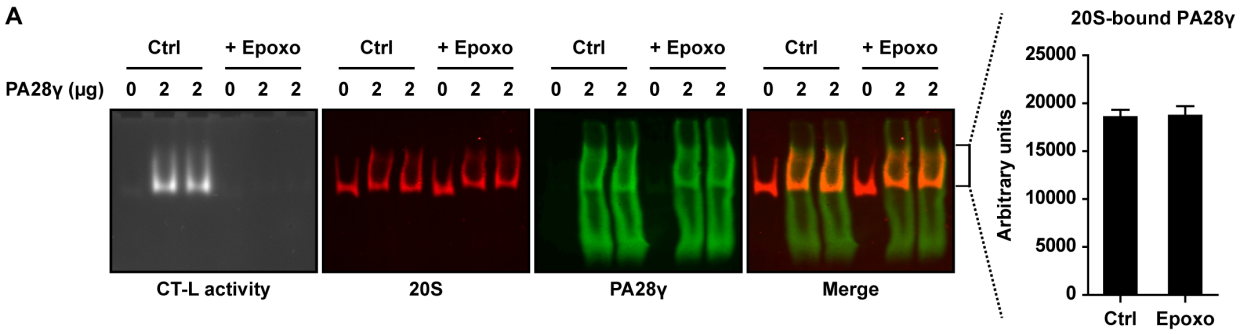

Figure 8

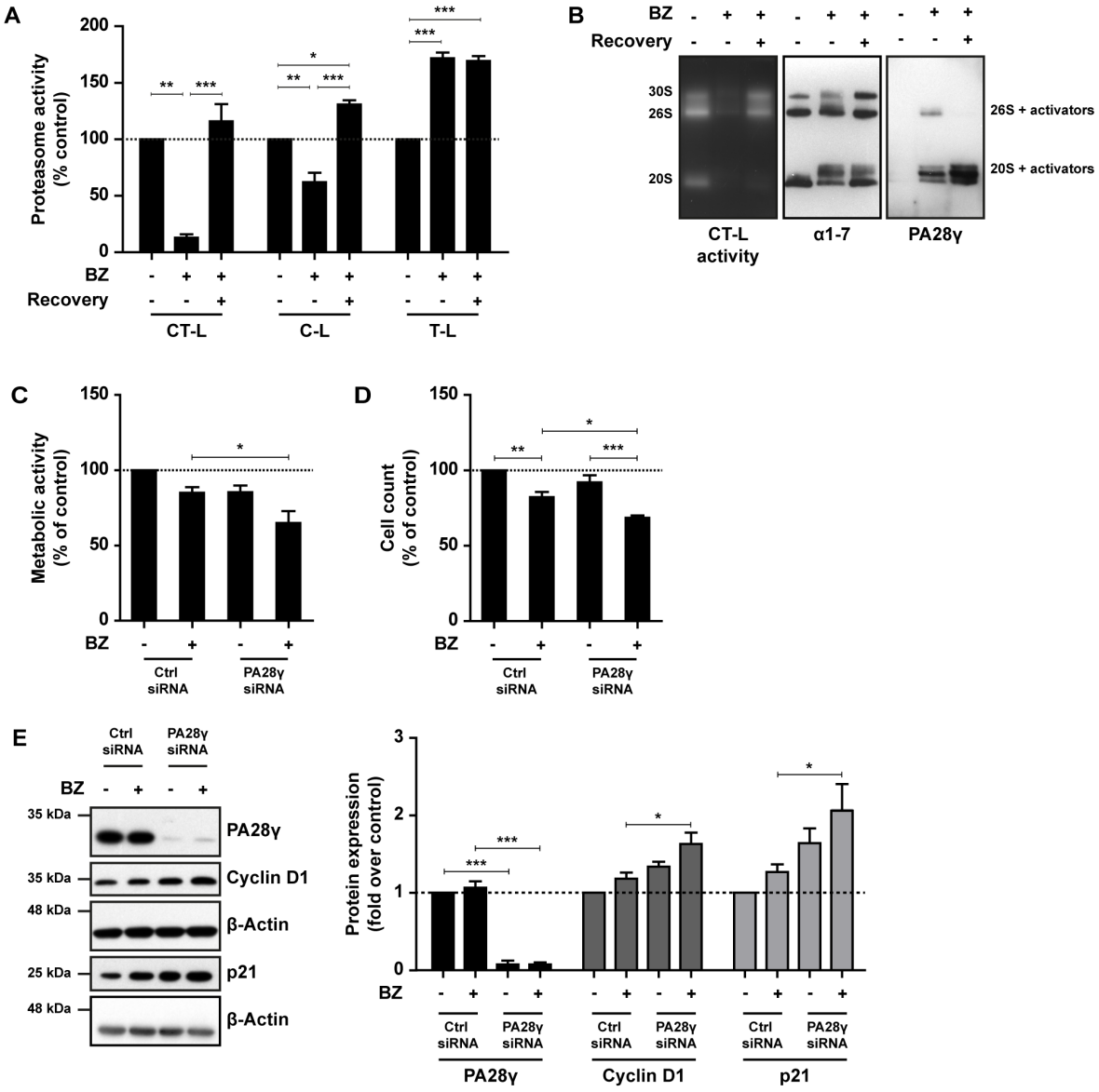

Inhibition of Proteasome Activity Induces Formation of Alternative Proteasome Complexes

Vanessa Welk, Olivier Coux, Vera Kleene, Claire Abeza, Dieter Truembach, Oliver Eickelberg and Silke Meiners

J. Biol. Chem. published online April 18, 2016
